frontiers in Marine Science

ORIGINAL RESEARCH
published: 19 February 2020
doi: 10.3389/fmars.2020.00059

Invasive *Spartina anglica* Greatly Alters the Rates and Pathways of Organic Carbon Oxidation and Associated Microbial Communities in an Intertidal Wetland of the Han River Estuary, Yellow Sea

*Sung-Uk An, Hyeyoun Cho, Ui-Jung Jung, Bomina Kim, Hyeonji Lee and Jung-Ho Hyun**

Department of Marine Sciences and Convergent Technology, Hanyang University, Ansan, South Korea

Biogeochemical process studies and molecular microbiological analyses were applied to assess the effect of invasive *Spartina anglica* (SA) on organic carbon (C_{org}) oxidation pathways and microbial community structures in intertidal sediments vegetated by the indigenous marsh plant *Suaeda japonica* (SJ) and unvegetated mud flats (UMF). Invasive *S. anglica* possessed 10 times the below-ground biomass of native *S. japonica*, which was responsible for releasing a substantial amount of labile dissolved organic matter and creating relatively oxidized conditions at the SA site. As a result, microbial metabolic activities measured by rates of anaerobic C_{org} oxidation, iron reduction (FeR) and sulfate reduction (SR) appeared to be greater at SA site compared with the SJ and UMF sites. SR was the dominant anaerobic respiration pathway at a depth of 0–10 cm for vegetated sediments, but the contribution of FeR to C_{org} oxidation was exceptionally high in the rhizosphere of the vegetated sites, comprising 60% and 70% of anaerobic C_{org} oxidation of SA and SJ, respectively. The iron turnover rate at the rhizosphere was 3 times higher at SA site (0.063 d^{-1}) compared with the SJ site (0.023 d^{-1}), indicating that the denser root system of invasive *S. anglica* greatly accelerates iron cycling. Bacterial communities based on 16S rRNA genes analysis revealed that members in *Desulfuromonadaceae* related to the reduction of FeOOH and S^0 were highly abundant at the relatively oxidized SA site, whereas *Desulfobulbaceae,* which are known as sulfate reducers, were more dominant at the relatively reduced SJ site. Similarly, two sulfur-oxidizing bacteria groups with different eco-physiological strategies thrived in each of the two vegetated sites. *Thioprofundaceae* in the *Gammaproteobacteria* were the predominant S-oxidizers at the less-reduced SA site, whereas *Sulfurovum* in the *Epsilonproteobacteria* dominated at the relatively reduced SJ site. Our results suggest that an invasion of tall *S. anglica* and its subsequent displacement of native *S. japonica* would greatly alter the biogeochemical C–Fe–S cycles and associated microbial communities, which ultimately generate multidirectional variations in ecological and biogeochemical processes in coastal ecosystems.

Keywords: biological invasion, *Spartina anglica*, *Suaeda japonica*, organic carbon oxidation, iron reduction, sulfate reduction, intertidal wetland, Yellow Sea

OPEN ACCESS

Edited by:
Mark James Hopwood, GEOMAR Helmholtz Centre for Ocean Research Kiel, Germany

Reviewed by:
Yongxin Lin, Fujian Normal University, China
Jiangtao Li, Tongji University, China

***Correspondence:**
Jung-Ho Hyun
hyunjh@hanyang.ac.kr

Specialty section:
This article was submitted to Marine Biogeochemistry, a section of the journal Frontiers in Marine Science

Received: *18 September 2019*
Accepted: *27 January 2020*
Published: *19 February 2020*

Citation:
An S-U, Cho H, Jung U-J, Kim B, Lee H and Hyun J-H (2020) Invasive Spartina anglica Greatly Alters the Rates and Pathways of Organic Carbon Oxidation and Associated Microbial Communities in an Intertidal Wetland of the Han River Estuary, Yellow Sea. Front. Mar. Sci. 7:59. doi: 10.3389/fmars.2020.00059

INTRODUCTION

Organic materials deposited in marine sediments are quickly mineralized by hydrolysis, fermentation, and a variety of processes that use different terminal-electron acceptors, including O_2, NO_3^-, Mn(IV), Fe(III), and SO_4^{2-} (Froelich et al., 1979; Canfield et al., 2005; Jørgensen, 2006). In organic-rich coastal sediments, where oxygen penetration is limited to a depth of a few mm, sulfate reduction (SR) dominates the anaerobic organic carbon (C_{org}) oxidation process (Howarth and Giblin, 1983; Hines et al., 1989). However, in coastal areas where rapid iron cycling occurs, microbial Fe(III) reduction (FeR) becomes a significant anaerobic C_{org} oxidation pathway (Kostka et al., 2002a,b; Jensen et al., 2003; Hyun et al., 2007, 2009; Kristensen et al., 2011). Because of the abundance and highly reactive properties of iron and sulfur in marine sediments, the partitioning of C_{org} oxidation by FeR and SR has a profound influence on the distribution and behavior of redox-sensitive metals and nutrients (Jensen et al., 1995; Dollhopf et al., 2005; Quintana et al., 2015; An et al., 2019; Mok et al., 2019). Therefore, elucidation of the relative significance of FeR and SR in C_{org} oxidation can improve our understanding of biogeochemical processes in sediments (King et al., 2001; Koretsky et al., 2003; Hyun et al., 2009; Luo et al., 2016; An et al., 2019).

In sediment that experiences rapid turnover of elements, the dynamics (i.e., production or consumption) of chemical constituents can hardly be interpreted by geochemical analyses alone (Jørgensen, 2006). In such conditions, the composition and diversity of microbial communities are among the most sensitive and rapid bio-indicators of environmental change because microorganisms with fast growth rates respond quickly to changes in environmental conditions (Lovell, 2005; Bertics and Ziebis, 2009; Choi et al., 2018). Therefore, it is highly relevant to combine biogeochemical process analysis with microbiological information to confirm if certain C_{org} oxidation pathways occur or dominate under specific conditions, where the geochemical evidence is less informative in complex environments (Weiss et al., 2003; Dollhopf et al., 2005; Vandieken et al., 2012; Choi et al., 2018).

Intertidal sediments in coastal ecosystems are biogeochemical hot spots where organic material and inorganic nutrients turn over rapidly along the land-sea continuum (Alongi, 1998; Odum, 2000; Cook et al., 2004; Hyun et al., 2009; McLeod et al., 2011). In this respect, the Ganghwa intertidal wetland in Gyeonggi-Incheon Province in the mid-west of the Korean peninsula (**Figure 1a**) is a significant environmental buffer, mineralizing organic matter that arrives via the Han River, which passes through the Seoul-Gyeonggi-Incheon metropolitan area, where more than 25 million people reside (Hyun et al., 2009). The native marsh plant *Suaeda japonica* (**Figures 1b,d**), which has thrived extensively in this area, plays a significant role in regulating the rates and pathways of C_{org} oxidation (Hyun et al., 2009). However, since it was first reported in the area in 2015, the invasive plant *Spartina anglica* C. E. Hubbard has rapidly displaced native *S. japonica* (**Figures 1b,c**), expanding its coverage by a factor of 80 from approximately 400 m^2 in 2015 to 31,181 m^2 in 2018 (KOEM, 2018). *Spartina* species, due to their relatively greater biomass, longer growing season, and higher photosynthetic rate compared with native species, are regarded as competitive invaders (Liao et al., 2007; Jiang et al., 2009; Li et al., 2009). Because biogeochemical processes in sediment are directly or indirectly coupled with the oxidation of organic materials (Fenchel et al., 1998; Canfield et al., 2005), it is particularly important to determine the rates and partitioning of C_{org} oxidation to better evaluate the impact of an invasive plant on biogeochemical processes in coastal ecosystems.

Previous studies have reported that invasion of *Spartina* species remarkably altered sedimentary biogeochemical cycles (Liao et al., 2007; Cheng et al., 2008; Zhang et al., 2017; Wang et al., 2019), physico-chemical properties of sediment (Yang et al., 2013; Bu et al., 2015; Zhang et al., 2019), and microbial communities in sediments associated with nitrification and denitrification (Dollhopf et al., 2005; Zhang et al., 2013; Gao et al., 2019), sulfur-oxidizing and reducing processes (Thomas et al., 2014; Cui et al., 2017) and CH_4 emissions (Yuan et al., 2016). However, little is known about the impact of these invading salt marsh plants on biogeochemical processes and associated microbial communities in the Ganghwa intertidal flats of the Han River estuary in the Yellow Sea. The objectives of this study were: (1) to evaluate the impact of invasive *S. anglica* on sediment biogeochemistry, with a special emphasis on the rates and partitioning of C_{org} oxidation coupled with FeR and SR; and (2) to elucidate major microbial consortia associated with the major biogeochemical processes in the rhizosphere of the two vegetated sediments. Our biogeochemical process studies, combining comprehensive geochemical analysis and microbial metabolic rate measurements with molecular microbiological analysis, revealed that the expansion of invasive *S. anglica* has profound impacts on biogeochemical C–Fe–S cycles and associated microbial communities in the Ganghwa intertidal wetlands.

MATERIALS AND METHODS

Study Area

The Ganghwa intertidal wetland, with an area of 244 km^2 (**Figure 1a**; Woo and Je, 2002), represents the largest portion of the intertidal mud flats (875 km^2) in the mideastern portion of the Yellow Sea[1]. An exceptionally large tidal range (±6.5 m on average) exposes extensive intertidal areas during low tide. Invasive *S. anglica* in Ganghwa intertidal sediment shows rapid growth from May to August, exceeding heights of 1 m (**Figure 1c**), and typically flowers from September to October (Kim et al., 2015; Kim, 2016). Several rhizomes connected to stems spread out in shallow sediment, and extend sideways or to depths of 20 cm or more. These species have a fibrous, radiate root system within the top 10 cm of the surface sediment (Kim et al., 2015). Native *S. japonica,* in contrast, are highly salt-tolerant annual plants, and flower from August to September (Bang and Lee, 2019). They can reach a height of approximately 20 cm (**Figure 1d**), and major rhizospheres occur between

[1]http://www.kosis.kr

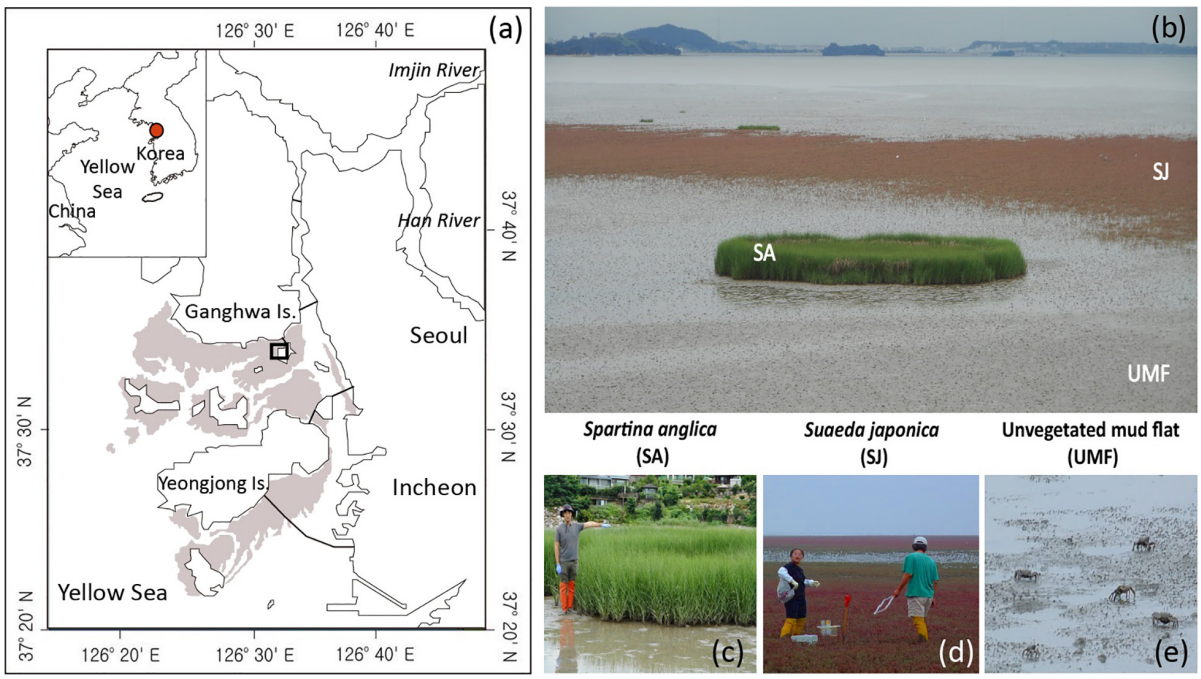

FIGURE 1 | A map showing sampling sites inhabited by *Spartina anglica* (SA) and *Suaeda japonica* (SJ) and the unvegetated mud flat (UMF) of the Ganghwa intertidal wetland **(a,b)**. Shaded area and the lines between land and island in **(a)** denote the intertidal wetlands and bridges, respectively. Note that the height of the SA shoot reaches 170 cm **(c)** whereas that of the SJ reaches approximately 30 cm **(d)**. Crabs (*Macrophthalmus japonicus*) are the dominant macrofauna in the UMF site **(e)**.

depths of 3 and 8 cm. In vegetated sediments, most burrowing activity occurs in shallow sediment, and burrows are generally smaller than those found in unvegetated areas because the roots of actively growing plants prevent burrowing activity of macrofauna (Gribsholt and Kristensen, 2003; Koo et al., 2007). In unvegetated mud flats, bioturbation by various macrofauna, such as crabs (*Macrophthalmus japonicus*) (**Figure 1e**) and worms (*Perinereis aibuhitensis*), plays a significant role in replenishing oxidants in sediment deeper than 30 cm (Koo et al., 2005, 2007; Hyun et al., 2009).

Sampling and Handling

Sediment samples for biogeochemical analysis, molecular microbiological analysis and metabolic rate measurements were collected on September 19, 2017, at three contrasting sites: (1) sediments inhabited by exotic *S. anglica* (Site SA); (2) sediments inhabited by the indigenous salt marsh plant *S. japonica* (Site SJ); and (3) unvegetated mud flats (Site UMF) (**Figure 1**). Sampling was performed randomly at a few cm away from plant shoots or burrows at all sites. Sediment samples for geochemical analysis were taken in triplicate from each site using acrylic cores (40 cm length, 6 cm internal diameter) that were immediately sealed with butyl rubber stoppers. Within 3 h of sampling, the cores were transferred to a N_2-filled glove bag (AtmosBag, Sigma-Aldrich Ltd., United States), and sectioned in the laboratory at 2 cm intervals down to a depth of 14 cm, and then at 4 cm intervals down to 30 cm. Sectioned sediments were transferred into polypropylene conical tubes in the same N_2-filled glove bag. The tubes were then tightly capped and sealed with rubber tape, and centrifuged at 2,600 *g* for 10 min. After reintroduction to the N_2-filled glove bag, supernatant pore water was sampled from the top and filtered through a 0.2 μm cellulose acetate syringe filter (Advantec, Toyo Rashi Kaisha, Ltd., Japan). To determine NH_4^+ and PO_4^{3-} concentrations, aliquots of 1–2 mL of pore water were frozen until analysis. To determine the dissolved Fe^{2+} and SO_4^{2-}, 2 mL of pore water was preserved with 12 N HCl (final conc. 0.1 N) and then stored at 4°C. Dissolved sulfide (H_2S) was precipitated with a zinc acetate solution (20%) and kept frozen. Pore-water was extracted using Rhizon samplers (Rhizosphere Research Products B.V, Wageningen, Netherlands) at depth intervals of 0–4, 4–8, 8–12, and 12–20 cm for an analysis of dissolved organic carbon (DOC). To prevent microbial activity, the DOC samples were acidified to a pH < 2 with 6 M HCl and preserved at 4°C until further analysis. Sediment samples for solid-phase analysis were kept frozen until processed in the laboratory. Additional sediment samples were collected to determine the major microbial communities associated with iron and sulfur cycles in the rhizosphere of the two vegetated sites. Two sediment cores of each *Spartina* and *Suaeda*, were collected using acrylic cores (40 cm length, 6 cm internal diameter). The rhizosphere within the sediment core was easily identified by the clusters of rhizome (**Figure 2**). The sediment loosely attached to the root was carefully scraped off from rhizosphere layer using a sterilized spatula, mixed well in the sterilized plastic bag, and immediately frozen at −80°C.

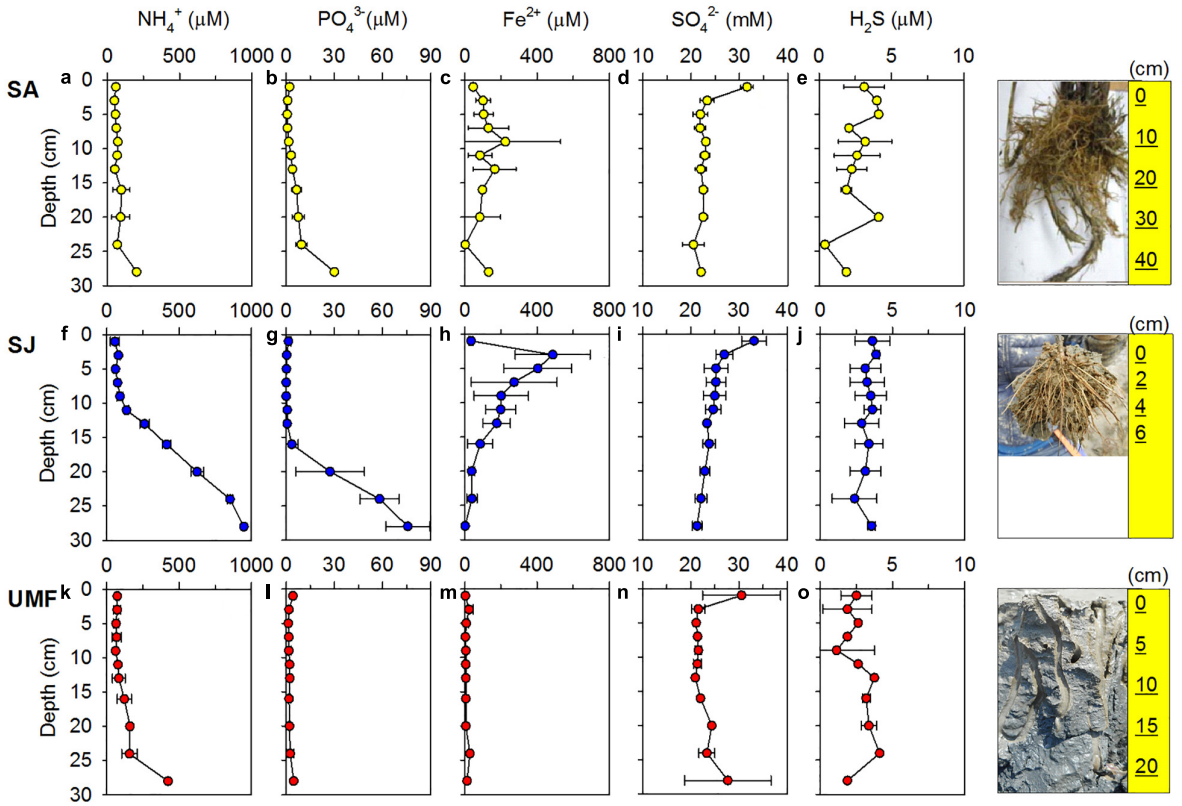

FIGURE 2 | Vertical profiles of NH_4^+ **(a,f,k)**, PO_4^{3-} **(b,g,l)**, Fe^{2+} **(c,h,m)**, SO_4^{2-} **(d,i,n)**, and H_2S **(e,j,o)** in the pore water at the *Spartina anglica* (SA), *Suaeda japonica* (SJ) sites and the unvegetated mud flat (UMF) site. Error bars indicate a mean ± 1 SD from duplicate or triplicate cores. The rightmost figures indicate the size of root systems of *S. anglica* and *S. japonica*, and the burrows formed by macrofauna in the UMF site.

Pore-Water Analysis

Dissolved NH_4^+ and PO_4^{3-} in pore water were measured using a continuous-flow nutrient analyzer (QuAAtro, Seal Analytical GmbH, Norderstedt, Germany), and a certified reference material from MOOS-3 (National Research Council, Canada) was included in each batch of nutrient samples. Reproducibility was generally within ±7%. Dissolved Fe^{2+} in pore water was determined by colorimetry with a ferrozine solution (detection limit: 1 μM; Stookey, 1970). SO_4^{2-} concentration was measured using ion chromatography (detection limit: 0.03 mM; 819 IC detector using an A-Supp5 column, Metrohm, Swiss). H_2S in the pore water was determined using methylene blue (detection limit: 3 μM; Cline, 1969). The concentrations of pore-water DOC were measured using a TOC-V_{CPH} analyzer (Shimadzu, Japan).

Solid-Phase Analysis

Total oxalate-extractable Fe, hereafter $TFe_{(oxal)}$, was extracted from air-dried sediment in a 0.2 M oxic oxalate solution (pH 3) for 4 h (Thamdrup and Canfield, 1996), while oxalate-extractable Fe(II), hereafter $Fe(II)_{(oxal)}$, was extracted from frozen sediment in anoxic oxalate (Phillips and Lovley, 1987). The $TFe_{(oxal)}$ and $Fe(II)_{(oxal)}$ were determined as described for the pore-water analysis of Fe^{2+}. Oxalate-extractable Fe(III), hereafter $Fe(III)_{(oxal)}$, was calculated from the difference between $TFe_{(oxal)}$ and $Fe(II)_{(oxal)}$. This fraction represents amorphous or poorly crystalline Fe(III) forms (Kostka and Luther, 1994). Total reduced inorganic sulfur (TRIS) in the sediments, which included both acid-volatile sulfide (AVS = FeS + H_2S) and chromium-reducible sulfur (CRS = S^0 + FeS_2), was determined after two-step distillation with cold 12 M HCl and boiling 0.5 M Cr^{2+} solution (Fossing and Jørgensen, 1989), and sulfide was determined according to the method of Cline (1969). Elemental sulfur (S^0) that is the sulfur extracted with methanol (high-performance liquid chromatography [HPLC] grade) from sediment samples was measured as cyclo-S_8 by reversed-phase HPLC (Zopfi et al., 2004). The content of particulate organic carbon (POC) and total nitrogen (TN) was analyzed using a vario PYRO cube elemental analyzer (Elementar Analysensysteme GmbH, Germany) after removal of $CaCO_3$. Chlorophyll *a* (Chl-a) concentrations in surface sediment (0–2 cm) were determined using spectrophotometry according to Parsons et al. (1984).

Rates of Anaerobic Carbon Oxidation, Iron Reduction and Sulfate Reduction

To determine anaerobic C_{org} oxidation rates and dissimilatory Fe(III) reduction rates (FeRR), sediment from a depth of 0–10 cm was collected using acrylic cores (20 cm length, 10 cm internal diameter) that were immediately sealed with butyl rubber

stoppers. Sediment cores were transferred to a N_2-filled glove bag and sliced in 2 cm intervals to a depth of 10 cm. Sediment was homogenized and loaded into 50 mL centrifuge tubes and these tubes were incubated at *in situ* temperatures (ca. 20–22°C) in the dark. At regular intervals, two tubes were sacrificed and the pore waters were extracted by centrifugation and filtered as described above in sediment handling. For total dissolved inorganic carbon (DIC) analysis, we collected 1.8 mL aliquots in glass vials without head space, fixed with 18 μL of saturated $HgCl_2$ (125 mM), and analyzed them as soon as possible using flow injection analysis with conductivity detection (detection limit for DIC is 1 mM; Hall and Aller, 1992). Anaerobic C_{org} oxidation rates were determined from the linear regression of the DIC accumulation with time. After pore-water retrieval from the anaerobic C_{org} mineralization incubation experiment, the remaining sediment was homogenized under a N_2 atmosphere, and Fe(II) was extracted in oxalate as described above in solid-phase analysis. FeRRs were determined by linear regression of the increase in solid-phase $Fe(II)_{(oxal)}$ content with time during incubations for the anaerobic C_{org} oxidation (Kostka et al., 2002a; Hyun et al., 2017).

Sulfate reduction rates (SRRs) were determined using the radiotracer method of Jørgensen (1978). Duplicate or triplicate intact cores (20 cm long with 2.5 cm i.d.) were collected at each site. Two μCi of $^{35}S\text{-}SO_4^{2-}$ (NEX041H005MC, PerkinElmer, United States) were injected into the injection port at 1 cm intervals, and the cores were incubated for 1–2 h at *in situ* temperatures. The sediment was sliced into sections, fixed in zinc acetate (20%), and frozen until processed in the laboratory. The reduced ^{35}S was recovered using distillation with a boiling acidic Cr^{2+} solution according to Fossing and Jørgensen (1989). The radioactivity of the reduced ^{35}S was quantified using a liquid scintillation counter (Tri-Carb 2910 TR; PerkinElmer, Waltham, MA, United States). SRR detection limits estimated from double-standard deviation of the blank value (Fossing et al., 2000) ranged from 0.72 to 5.75 nmol cm^{-3} d^{-1}.

Partitioning of Organic Carbon Oxidation

The relative significance of FeR and SR in anaerobic C_{org} oxidation was estimated after converting the FeR and SR to carbon units (see Hyun et al., 2017). Briefly, to calculate the C_{org} oxidation by microbial FeR, the 4Fe: 1C stoichiometry of FeR coupled with C_{org} oxidation was used from the stoichiometric equation (Canfield et al., 1993): $CH_2O + 4FeOOH + 8H^+ = CO_2 + 4Fe^{2+} + 7H_2O$. To calculate the contribution of SR in anaerobic carbon oxidation, the SRRs were converted to carbon oxidation using a stoichiometric equation (Thamdrup and Canfield, 1996): $2CH_2O + SO_4^{2-} + 2H^+ = 2CO_2 + H_2S + 2H_2O$.

DNA Extraction, Sequencing, and Sequence Analyses

To support the results on biogeochemical process associated with Fe–S cycles in the rhizosphere, additional microbial community analysis was conducted using a sediment core collected at SA and SJ. Total genomic DNA was extracted using a Powersoil DNA Isolation kit (Mo Bio Laboratories, Carlsbad, CA, United States), following the manufacturer's instructions. 16S rRNA genes amplification for sequencing was performed with the primers containing the Illumina adaptor sequences and universal V3-V4 region of the 16S rRNA gene (341F: CCTACGGGNGGCWGCAG and 805R: GACTACHVGGGTATCTAATCC). Sequencing of 16S rRNA gene amplicons was performed by the Illumina MiSeq platform at Macrogen Inc. (Seoul, South Korea) according to the manufacturer's instructions. Sequences were clustered into operational taxonomic units (OTUs), which met a 97% similarity threshold, using the multi-step pipeline CD-HIT-OTU tool and rDnaTools (Schloss et al., 2009; Li et al., 2012). Chimeric sequences were identified and removed by rDnaTools. The 16S rRNA gene sequences were identified by comparing the datasets against the Ribosomal Database Project (RDP) Classifier tool. Alpha diversity indices were created using QIIME software (Caporaso et al., 2010). Raw sequence data have been submitted to the National Center for Biotechnology Information under study accession number PRJNA565620.

Plant Biomass

Above- and below-ground biomass (AGB and BGB, respectively) and shoot density of both *S. anglica* and *S. japonica* was determined by harvesting all materials in five randomly selected 25 × 25 cm^2 frames. Plant shoots for measuring AGB were cut at the sediment surface, and the sediment for estimating BGB were moved to the laboratory. The plant materials and detritus were washed carefully with tap water and rinsed twice with distilled water. Belowground tissues were washed using 500 μm sieve to avoid the loss of small roots. They were separated into leaves, stems and below-ground material, and then dried at 60°C for > 48 h to determine dry weight.

Data Analysis

Depth-integrated analysis was conducted for the quantitative comparison of geochemical parameters and rate measurements at the SA, SJ, and UMF sites. A one-way analysis of variance was performed to identify significant differences among different sampling sites. Tukey's honestly significant difference *post hoc* test was used to determine statistically significant differences between stations. If homogeneity of variances (Levene's test) were not obtained, a non-parametric Kruskal–Wallis test was used, both at a critical level of 0.05. Statistical analyses were performed using SPSS ver. 21 (SPSS for Windows, SPSS, Inc.).

RESULTS

Sediment Properties

Physico-chemical and ecological properties obtained at the three sampling sites are presented in **Table 1**. Porosity ranged from 0.56 to 0.61, and water content varied from 33.9 to 35.9% among the sites. POC and TN in the sediments ranged from 0.72 to 1.01%, and 0.11 to 0.12%, respectively. The POC at SA patch was slightly higher than those of other sites. The above- and below-ground biomass at SA patch (AGB = 2021 g m^{-2}, BGB = 1358 g m^{-2})

TABLE 1 | Physico-chemical and ecological parameters in the surface sediments (0–10 cm).

	Sites		
	SA	**SJ**	**UMF**
Physico-chemical properties			
Porosity*	0.61 (± 0.02)^{a}	0.59 (± 0.03)^{a,b}	0.56 (± 0.04)^{b}
Density (g cm^{-3})*	1.71 (± 0.07)^{a}	1.63 (± 0.04)^{b}	1.64 (± 0.07)^{b}
Water content (%)	35.5 (± 2.34)	35.9 (± 2.81)	33.9 (± 2.31)
POC (% dry wt)§	1.01 (± 0.08)	0.72 (± 0.07)	0.80 (± 0.08)
TN (% dry wt)§	0.11 (± 0.01)	0.11 (± 0.01)	0.12 (± 0.01)
Ecological properties			
Aboveground biomass (AGB, g m^{-2})	2, 021 (± 835)	281 (± 84.9)	–
Belowground biomass (BGB, g m^{-2})	1, 358 (± 365)	138 (± 25.8)	–
Shoot density (shoots m^{-2})	268 (± 52.3)	201 (± 94.4)	–
Sediment Chl-*a* (mg m^{-2})§	114 (± 20.3)	92.0 (± 7.91)	113 (± 0.72)

Values represent the mean ± SD. §*Average concentration at 0–2 cm depth interval. *The asterisks indicate a significant difference between stations with $p < 0.05$. Superscript letters indicate significant differences ($p < 0.05$) between homogeneous groups (ANOVA, post hoc Tukey HSD test) for a specific variable.*

TABLE 2 | Depth-integrated inventories (mmol m^{-2}) of pore-water constituents and solid-phase constituents (n = 3).

	Parameter	Sites		
		SA	**SJ**	**UMF**
Pore- water	NH_4^{+}*	16.4^{a}	84.2^{b}	25.5^{a}
	PO_4^{3-}	1.49	3.67	0.44
	Fe^{2+}*	22.3^{a}	23.1^{a}	1.19^{b}
	SO_4^{2-}	4144	4223	4005
	HS^{-}	0.46	0.56	0.47
	DOC*	560^{a}	258^{b}	192^{b}
Solid- phase	$Fe(II)_{(oxal)}$*	8016^{a}	6929^{a}	2728^{b}
	$Fe(III)_{(oxal)}$*	14085^{a}	14209^{a}	24438^{b}
	AVS	15.9	25.4	29.1
	CRS*	4198^{a}	2690^{b}	2597^{b}
	S^{0}*	239^{a}	104^{b}	70.3^{b}

Depth integration for each parameter was made down to the depth appeared in ***Figures 2–4****. *The asterisks indicate a significant difference between stations with $p < 0.05$. Superscript letters indicate significant differences ($p < 0.05$) between homogeneous groups (ANOVA, post hoc Tukey HSD test) for a specific variable.*

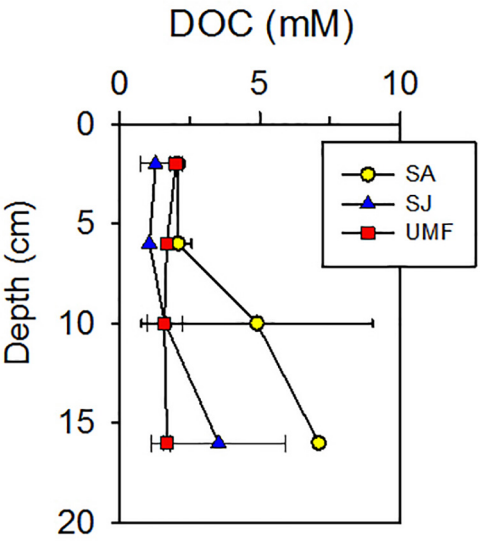

FIGURE 3 | Vertical profiles of dissolved organic carbon (DOC) in sediment vegetated by *Spartina anglica* (SA) and *Suaeda japonica* (SJ) and unvegetated mud flats (UMF). Error bars indicate a mean ± 1 SD from triplicate cores.

were 7- and 10-fold, respectively, greater than that of SJ patch (AGB = 281 g m^{-2}, BGB = 138 g m^{-2}).

Pore-Water Constituents

NH_4^{+} concentrations at SA and UMF sites were constantly low at entire depth (**Figures 2a,k**), whereas it increased steeply below 10 cm depth at SJ (**Figure 2f**). The depth-integrated concentration (0–30 cm) of NH_4^{+} at SJ site was 3.3- and 5.1-fold higher than at UMF and SA sites, respectively ($F_{2,30}$ = 8.73, p = 0.001; **Table 2**). PO_4^{3-} in the pore water showed similar vertical distribution patterns with the NH_4^{+} concentrations (**Figures 2b,g,l**). The depth-integrated concentrations of PO_4^{3-} were 2.5- and 8.3-fold higher at SJ than at SA and UMF, respectively, although the difference was not significant (p = 0.182; **Table 2**). Dissolved Fe^{2+} concentrations differed greatly among the sites (p = 0.001; **Table 2**). The highest Fe^{2+} concentration (486 μM) was observed at a depth of 2–4 cm at the SJ site (**Figure 2h**), and the concentration decreased below 1.80 μM at a depth of 26–30 cm. The Fe^{2+} peak (225 μM) observed at the 8–10 cm depth of SA site (**Figure 2c**) decreased slightly with increasing depth, whereas the Fe^{2+} concentrations were low at all depths at UMF site (**Figure 2m**). Depth-integrated inventories of Fe^{2+} at SA and SJ were 19 times greater than at UMF site (**Table 2**). SO_4^{2-} concentrations were similar (>21 mM) between the three sites (**Figures 2d,i,n**). Dissolved sulfide concentrations were close to the detection limit (<3 μM) at all sites (**Figures 2e,j,o**). SO_4^{2-} and H_2S concentrations did not differ significantly between the sites (p = 0.34 and p = 0.19,

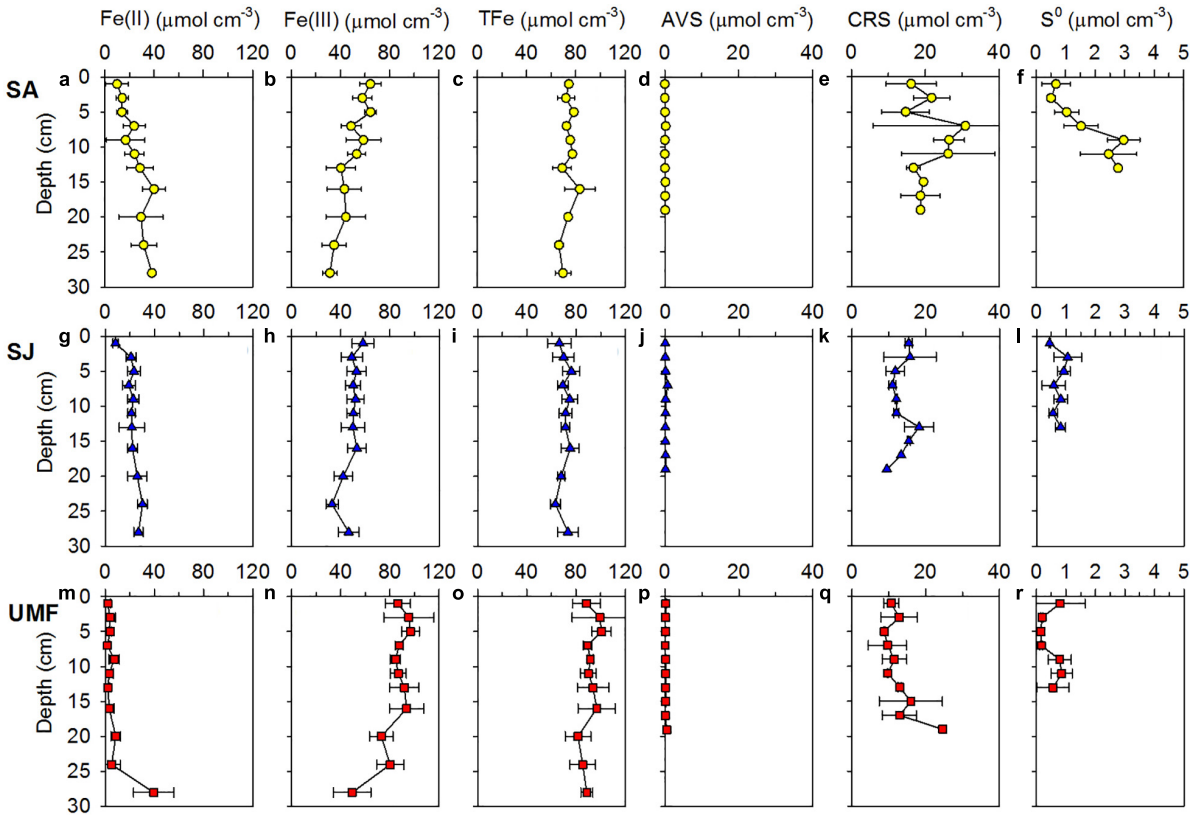

FIGURE 4 | Vertical profiles of oxalate-extractable Fe(II) **(a,g,m)**, Fe(III) **(b,h,n)**, total Fe (TFe) **(c,i,o)**, acid-volatile sulfur (AVS) **(d,j,p)**, chromium-reducible sulfur (CRS) **(e,k,q)**, and elemental sulfur (S^0) **(f,l,r)** in sediment vegetated by *Spartina anglica* (SA) and *Suaeda japonica* (SJ) and unvegetated mud flats (UMF). Error bars indicate the mean ± 1 SD from duplicate or triplicate cores.

respectively). Pore-water DOC at the SA site was constantly within 6 cm, but increased rapidly with depth from 7.1 mM at 16 cm depth (**Figure 3**). At SJ site, DOC concentrations increased slightly with increasing depth from 1.3 mM to 3.5 mM, whereas UMF was almost constant with depth (**Figure 3**).

Solid-Phase Iron and Sulfur

Vertical distributions of solid-phase iron and sulfur in sediment are presented in **Figure 4**. The concentrations of $Fe(II)_{(oxal)}$ increased slightly with depth at SA and SJ sites (**Figures 4a,g**), but $Fe(III)_{(oxal)}$ concentrations gradually decreased with increasing depth (**Figures 4b,h**). The $Fe(II)_{(oxal)}$ at UMF was lowest at all depths, except for 28–30 cm (**Figure 4m**). The depth-integrated (0–30 cm) amount of $Fe(III)_{(oxal)}$ was 1.7 times greater at UMF site than at other sites, and most solid-phase iron consisted of reactive Fe(III) (>60% of the total iron), which accounted for > 90% at UMF (**Table 2**). Most of the TRIS forms at the Ganghwa intertidal sediment was preserved in the CRS form (S^0 + FeS_2) (>95% of TRIS), while the concentrations of AVS (H_2S + FeS) were near depletion at all sites (<1 μmol cm^{-3}). CRS concentrations were almost constant with depth at all three sites, although small peak concentrations (26.2–30.9 μmol cm^{-3}) were observed at the 6–12 cm depth of SA site (**Figure 4e**). The depth-integrated (0–20 cm) CRS pool was greater at SA (4198 mmol m^{-2}) than at the other two sites (SJ; 2690 mmol m^{-2}, UMF; 2597 mmol m^{-2}) ($p < 0.001$; **Table 2**). S^0 concentration was more abundant at SA than SJ and UMF ($p < 0.05$; **Table 2**), and higher concentrations of S^0 were observed at the 8–14 cm depth at SA site (**Figure 4f**).

Rate Measurements

Depth-integrated (0–10 cm) anaerobic C_{org} oxidation at SA (88.7 mmol C m^{-2} d^{-1}) was two-fold greater than that of SJ (48.8 mmol C m^{-2} d^{-1}) and UMF sites (47.5 mmol C m^{-2} d^{-1}) (**Table 3**). Anaerobic C_{org} oxidation rates were highest at the rhizosphere (4–8 cm) of SA site (1183–1205 nmol C cm^{-3} d^{-1}), approximately 2–3 times higher than those measured at SJ (395–398 nmol C cm^{-3} d^{-1}) and at a depth similar to that of UMF (351–609 nmol C cm^{-3} d^{-1}) (**Figures 5a,d,g**). The depth-integrated (0–10 cm) FeRR at SA was twice as high as SJ and UMF site (**Table 3**). Similar to the anaerobic C_{org} oxidation rates, FeRRs were higher at the rhizosphere of SA (4–8 cm, 3084–3986 nmol Fe cm^{-3} d^{-1}) compared with that measured at SJ (468–931 nmol Fe cm^{-3} d^{-1}) and at a depth range similar to that of UMF site (912–1397 nmol Fe cm^{-3} d^{-1}) (**Figures 5b,e,h**). The depth-integrated (0–10 cm) SRR (29.0 mmol S m^{-2} d^{-1}) at SA was twice that at SJ (13.7 mmol S m^{-2} d^{-1}) and more than 4.4 times higher than at the UMF site (6.58 mmol S m^{-2} d^{-1}) (**Table 3**).

TABLE 3 | Partitioning of sulfate reduction (SRR) and Fe(III) reduction (FeRR) in C_{org} oxidation, and turnover rates of Fe(III).

Sites	Depth range (cm)	Anaerobic C_{org} oxidation rate (mmol C m^{-2} d^{-1})	SRR (mmol S m^{-2} d^{-1})	Total FeRR (mmol Fe m^{-2} d^{-1})	Abiotic FeRR[a]	Microbial FeRR	Contribution of C_{org} oxidation by[b]		Turnover rates of Fe(III)[c] (d^{-1})
							Sulfate Red. (%)	Iron Red. (%)	
SA	0–2	15.4	4.43	22.4	2.96	19.4	57.5	31.5	0.020
	2–4	13.0	7.02	14.2	4.68	9.53	108	18.3	0.015
	4–6	24.1	6.27	79.7	4.18	75.6	52.0	78.4	0.062
	6–8	23.7	5.58	61.7	3.72	58.0	47.1	61.2	0.063
	8–10	12.5	5.68	16.5	3.79	12.7	90.9	25.5	0.012
	Sum (0–10)	88.7	29.0	194	19.3	175	65.3	49.4	
SJ	0–2	10.9	2.44	21.7	1.63	20.0	45.0	46.1	0.019
	2–4	9.71	1.96	26.0	1.30	24.7	40.3	63.6	0.027
	4–6	7.97	1.85	18.6	1.23	17.4	46.4	54.6	0.018
	6–8	7.90	2.22	9.36	1.48	7.88	56.2	24.9	0.009
	8–10	12.4	5.27	8.74	3.51	5.22	85.2	10.6	0.008
	Sum (0-10)	48.8	13.7	84.4	9.16	75.2	56.3	38.5	
UMF	0–2	9.73	0.55	11.8	0.36	11.4	11.2	29.3	0.007
	2–4	5.59	0.96	17.8	0.64	17.2	45.8	76.8	0.009
	4–6	7.02	1.42	18.2	0.94	17.3	40.4	64.6	0.009
	6–8	12.2	2.93	20.6	1.95	18.6	48.1	38.3	0.016
	8–10	13.0	0.73	22.1	0.49	21.6	11.2	41.5	0.013
	Sum (0–10)	47.5	6.58	90.5	4.39	86.1	29.0	45.3	

[a] *Stoichiometric equations were used to evaluate the relative significance of abiotic and microbial Fe reduction: abiotic reduction of Fe(III) by sulfide oxidation,* $3H_2S + 2FeOOH = 2FeS + S^0 + 4H_2O$; *microbial FeRR = total FeRR - abiotic FeRR.* [b] *C mineralization by* SO_4^{2-} *reduction:* $SO_4^{2-} + CH_3COO^- + 2H^+ = 2CO_2 + 2H_2O + HS^-$, *C mineralization by microbial Fe(III) reduction:* $8FeOOH + CH_3COO^- + 17H^+ = 2CO_2 + 14H_2O + 8Fe^{2+}$. [c] *The turnover rate of Fe(III), as calculated from the FeRRs divided by the concentrations of* $Fe(III)_{(oxal)}$.

SRR at SA increased from 222 nmol m^{-3} d^{-1} at the surface to 453 nmol m^{-3} d^{-1} at 2–4 cm, and then decreased continuously to 65.8 nmol m^{-3} d^{-1} at a depth of 18 cm (**Figure 5c**), while the rates remained relatively constant with depth at SJ and UMF sites (**Figures 5f,i**).

Bacterial Communities

To further assess the impact of invasive *S. anglica* on biogeochemical processes, microbiological analyses of bacterial community structures were conducted at the rhizosphere of the SA and SJ sites. A total of 23,935 reads, with an average length of 440 base pairs, were obtained after excluding 865 sequences of the cyanobacterial 16S rRNA genes. Chao1 index and $OTU_{0.97}$ counts of bacterial 16S rRNA gene sequences were lower in the sediment at SA than at SJ. Of the 19 identified phyla of bacteria, *Proteobacteria*, comprising 71.9–79.5% of the total reads, represented the most predominant microbial group (**Figure 6** and **Table 4**). Among the *Proteobacteria, Deltaproteobacteria* (21.8–26.4%) and *Gammaproteobacteria* (43.7–44%) dominated both sites (**Figure 6** and **Table 4**). Bacteria belonging to *Bacteroidetes* appeared to be the second most dominant, comprising 13.2 and 8.53% of total reads at SA and SJ sites, respectively. Bacterial populations belonging to *Actinobacteria* (0.64–1.39%), *Firmicutes* (0.75–4.17%), *Fusobacteria* (1.26–3.59%), and *Verrucomicrobia* (0.57–1.50%) were minor bacterial groups (**Table 4**).

Major subgroups at the family level in *Deltaproteobacteria* and *Gammaproteobacteria* showed different distribution at SA and SJ sites (**Figure 6** and **Supplementary Table S1**). At SA, more than half of the deltaproteobacterial sequences (51.1% in the *Deltaproteobacteria*) were affiliated with *Desulfuromonadaceae*, including several iron-and elemental sulfur–reducing bacteria. The second dominant bacterial group in the deltaproteobacterial sequences was affiliated with *Desulfobulbaceae* (28.2% in the *Deltaproteobacteria*), which are well known as sulfate-reducing bacteria (**Figure 6**). In contrast, the relative contribution of *Desulfuromonadaceae*, thriving most abundantly at SA, appeared to be lower at SJ (32.2%) (**Figure 6**). Sulfate-reducing *Desulfobulbaceae* were more dominant at SJ (46.0% in the *Deltaproteobacteria*) than at SA (28.2%).

The distribution of major family groups for *Gammaproteobacteria* and *Epsilonproteobacteria* varied considerably with sites as well. Among *Gammaproteobacteria*, the family *Woeseiaceae*, facultatively anaerobic and heterotrophic marine bacteria (Du et al., 2016) were the most frequent at both sites, comprising 21.7–45.8% in total gammaproteobacterial sequences (**Figure 6**). The abundance of family *Thioprofundaceae* appeared to be the highest at SA (23.3% in the *Gammaproteobacteria*), but decreased to 7.52% at SJ (**Figure 6**). Likewise, members of the family *Halieaceae* in *Gammaproteobacteria* were also detected at a high proportion (12.8% in *Gammaproteobacteria*) at SA site, compared with those at SJ site (0.97%) (**Figure 6**). Meanwhile, the family *Psychromonadaceae* occupied the most abundant proportion in total gammaproteobacterial sequences (52%) at SJ (**Figure 6** and **Supplementary Table S1**). The relative abundance of *Sulfurovum* in *epsilonproteobacterial* sequences was higher at SJ (84.2% in *Epsilonproteobacteria*) compared with SA (66.8%) (**Supplementary Table S1**).

DISCUSSION

Influence of Invasive *S. anglica* on C_{org} Oxidation

The rates and pathways of C_{org} oxidation in sediments are largely regulated by the availability of electron donors (i.e., labile organic matters) and acceptors (Canfield et al., 2005). In coastal sediments, various physico-chemical and biological factors such as vegetation, bioturbation, freshwater runoff, tidal inundation, and anthropogenic activities are responsible for availability of the electron donors and acceptors for microbial metabolic activities (Alongi et al., 1999; Kristensen and Kostka, 2005; Hyun et al., 2009; An et al., 2019; Mok et al., 2019). Of all the environmental factors, marsh plants significantly affect biogeochemical properties by translocating organic matter via roots and rhizomes (Armstrong et al., 2000; Lee, 2003; Sundby et al., 2003; Koop-Jakobsen et al., 2018). For example, exudates from the roots of marsh plants provide bacteria with a large amount of labile organic carbon, enhancing microbial respiration in vegetated sediments (Hines et al., 1989; Gribsholt and Kristensen, 2002; Hyun et al., 2007). Furthermore, the rhizosphere appears to be a zone of intense re-oxidation of reduced solutes, such as Fe^{2+} and H_2S, which results in a rapid regeneration of Fe(III) and sulfate for re-stimulating FeR and SR, respectively (Hines et al., 1989; Gribsholt et al., 2003; Hyun et al., 2009; Luo et al., 2018).

In the present study, total anaerobic C_{org} oxidation rate, FeR, and SR were consistently higher at SA than at SJ and UMF (**Figure 4** and **Table 3**). Exceptionally enhanced metabolic activities were observed at the rhizosphere (4–8 cm depth) of SA. The results are consistent with previous studies conducted in salt marsh sediment vegetated by *Spartina* (Hines, 1991; Hines et al., 1994; Gribsholt et al., 2003; Luo et al., 2018). More than half of the photosynthetically fixed carbon by *S. anglica* is allocated in the below-ground root system (Hemminga et al., 1996). *Spartina* roots therefore provide substantial amounts of labile organic compounds (i.e., DOC) (Bu et al., 2015; Cheng et al., 2008; Zhang et al., 2017), which fuel anaerobic respiration in the sediment (Hines et al., 1989; Hines, 1991; Kostka et al., 2002a; Koretsky et al., 2008). Indeed, depth-integrated (0–20 cm) DOC concentrations at SA (560 mmol m^{-2}) were 2.2 times and 2.9 times higher than that measured at SJ (258 mmol m^{-2}) and UMF (192 mmol m^{-2}), respectively (**Table 2**). Specially, DOC concentrations at the rhizosphere depth (10–15 cm) of SA site were 3-times greater than that measured at the rhizosphere depth (3–6 cm) of SJ and at the entire depth of UMF sites (**Figure 3**). The results indicated that invasive *Spartina* species possessing 10 times the below-ground biomass of native *S. japonica* (**Figure 3** and **Table 1**) exudates more labile dissolved organic matter into sediments, thereby stimulating the microbial metabolic activities.

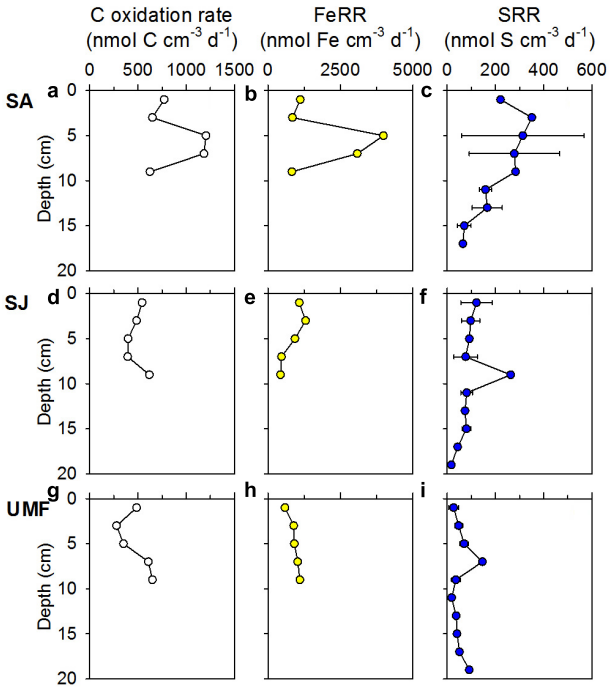

FIGURE 5 | Vertical profiles of anaerobic C_{org} oxidation rates **(a,d,g)**, iron reduction rates (FeRR) **(b,e,h)**, and sulfate reduction rates (SRR) **(c,f,i)** in the sediments vegetated by *Spartina anglica* (SA) and *Suaeda japonica* (SJ) and unvegetated mud flats (UMF). Error bars in SRR indicate the mean ± 1 SD from triplicate cores.

Partitioning of C_{org} Oxidation and Associated Microbial Communities in Rhizosphere

In addition to stimulating metabolic activities, the invasion of *S. anglica* in Ganghwa intertidal sediment exerted a profound influence on sediment biogeochemistry associated with the partitioning of C_{org} oxidation. SR appeared to be the dominant anaerobic respiration pathway at 0–10 cm depth of the vegetated SA and SJ sediments, comprising 65.3 and 56.3% of anaerobic C_{org} oxidation, respectively (**Table 3**). However,

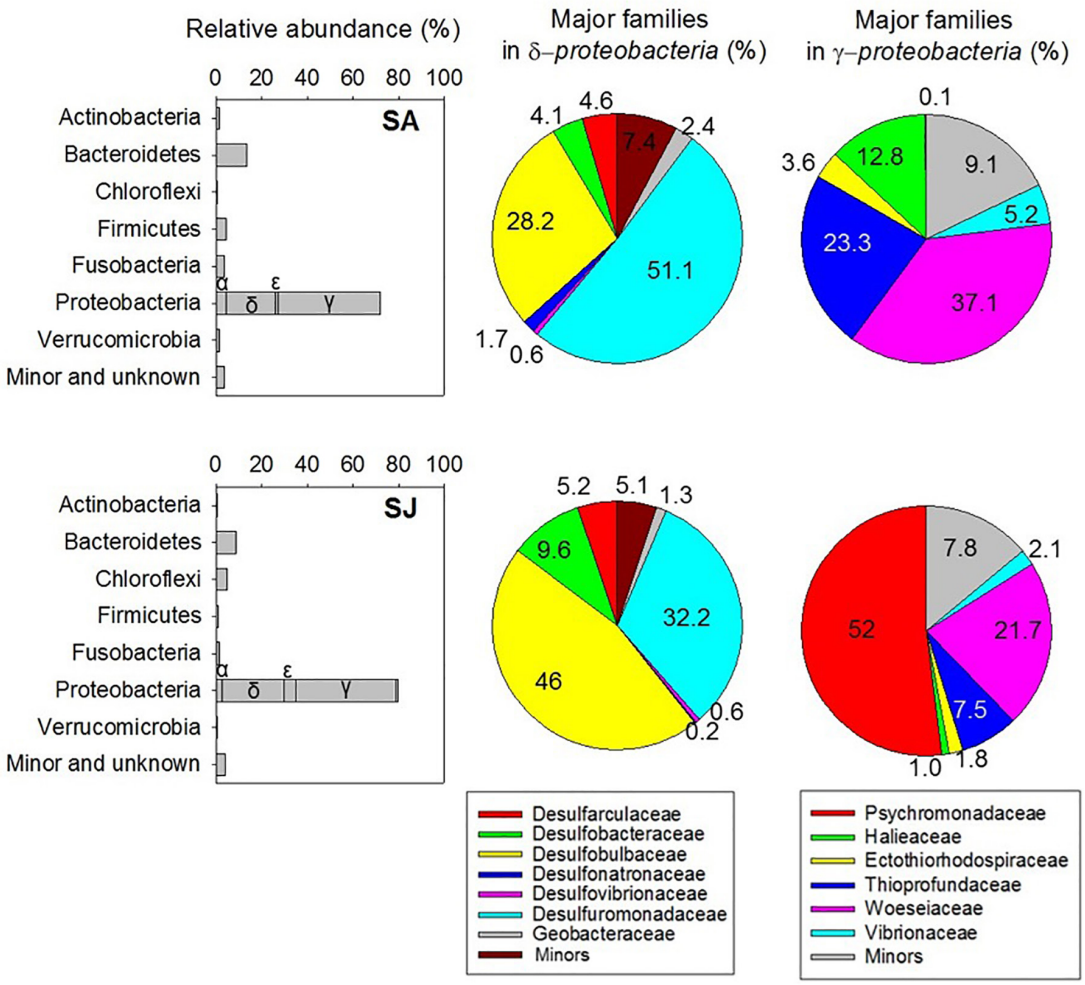

FIGURE 6 | Relative abundance of major bacterial phyla (bar chart) and families in *Delta-* and *Gammaproteobacteria* (pie chart) within a depth of 4–8 cm of the sediment inhabited by invasive *Spartina anglica* (SA) and native *Suaeda japonica* (SJ).

in the rhizosphere layers of SA (4–8 cm) and SJ (2–6 cm), the contribution of FeR to C_{org} oxidation was higher than that of the SR, comprising approximately 70 and 60% of anaerobic C_{org} oxidation, respectively (**Table 3**). Together with the exceptionally high FeR (**Figure 5b**), the higher contribution of FeR in C_{org} oxidation at the rhizosphere of SA indicated that the large root system of invasive *S. anglica* greatly accelerates iron cycling in the sediment. Indeed, the iron turnover rates at the rhizosphere depth of SA site (0.063 d^{-1} in average) were 3–5 times higher than that measured at the rhizosphere depth at SJ (0.023 d^{-1} in average) and UMF (0.013 d^{-1} in average), respectively (**Table 3**). In the Georgia salt marsh, Hyun et al. (2007) reported that FeR represented 21–69% of C_{org} oxidation due to rapid regeneration of Fe(III) by root of *S. alterniflora*. Gribsholt and Kristensen (2002) also found that FeR accounts for the majority of C_{org} oxidation in the mesocosms manipulated with *S. anglica* by supplying Fe(III) through downward translocation of oxygen, which leads to the re-oxidation of Fe(II).

The dominance of FeR in C_{org} oxidation at SA was further supported by the relative abundance of microbial consortia in the rhizosphere. At SA, the genera *Desulfuromonas*, *Pelobacter*, and *Desulfuromusa* in the family *Desulfuromonadaceae* among *Deltaproteobacteria* appeared to be the dominant bacterial groups. They reportedly oxidize organic matter using various electron acceptors such as Mn(IV), Fe(III), S^0, and $S_2O_3^{2-}$ in anoxic conditions (Liesack and Finster, 1994; Vandieken et al., 2006; Haveman et al., 2008). Considering that FeR is a dominant C_{org} oxidation pathway in the rhizosphere of SA (**Table 3**), supply of Fe(III) via rapid iron turnover in the presence of the extensive root system of *S. anglica* ultimately provides a favorable condition for Fe(III) reduction by *Desulfuromonadaceae*. The high abundance of *Desulfuromonadaceae* that use both Fe(III) and S^0 as electron acceptors was further supported by high S^0 concentrations in rhizosphere of SA (**Figure 4f**).

On the other hand, in unvegetated UMF site, Fe(III) appears to be the most influential electron acceptor for C_{org} oxidation

TABLE 4 | Phylogenetic composition and diversity indices of 16S rRNA genes in the 4–8 cm depth of the Ganghwa intertidal sediments.

Diversity indices	SA	SJ
Total reads	10401	13534
Observed OTUs	616	641
Chao1	661.7	733.5
Shannon	6.7	6.0
Simpson	1.0	0.9
Goods Coverage[a] (%)	99.2	99.0
Phylogenetic group (%)		
Acidobacteria	0.12	0.33
Actinobacteria	1.39	0.64
Bacteroidetes	13.2	8.53
Calditrichaeota	0.08	0.38
Chloroflexi	0.58	4.75
Firmicutes	4.17	0.75
Fusobacteria	3.59	1.26
Ignavibacteriae	0.04	0.25
Nitrospinia	0.07	0.18
Nitrospira	0.40	0.18
Planctomycetes	0.40	0.09
Proteobacteria	71.9	79.5
Alphaproteobacteria	4.18	3.06
Betaproteobacteria	0.37	0.25
Deltaproteobacteria	21.8	26.4
Epsilonproteobacteria	1.77	5.62
Gammaproteobacteria	43.7	44.0
Minors and unclassified proteobacteria	0.11	0.17
Spirochaetia	0.11	0.20
Verrucomicrobia	1.50	0.57
Minors and unknown	2.37	2.31

[a]*Good's coverage (%) = [1-(n/N)] × 100 (n, the number of OTUs; N, the total number of clones).*

(**Figure 4n**, **Table 2**). Accordingly, FeR accounted for 45.3% of anaerobic C_{org} oxidation, whereas SR only accounted for 29% (**Table 3**). The burrows constructed by macrofauna foster relatively oxidized conditions by increasing the area of the sediment-water interface at UMF site (Koo et al., 2007). Under these conditions, reactive Fe(III) is readily supplied via macrofaunal burrowing activities, thereby allowing FeR to outcompete SR in anaerobic C_{org} oxidation processes at UMF (**Table 3**, Gribsholt et al., 2003; Kristensen and Alongi, 2006).

Biogeochemical and Microbiological Evidence for a Profound Influence of *S. anglica* on Iron and Sulfur Cycles

Microbial metabolic activities by SR and FeR ultimately produce H_2S and Fe^{2+}, respectively (Eqs. 1–2). However, despite high SRR and FeRR at the rhizosphere of SA (**Figures 5b,c** and **Table 3**), H_2S in the pore water of SA was depleted (**Figure 2e**), and the accumulation of Fe^{2+} was smaller at SA site (**Figure 2c**) than at SJ site (**Figure 2h**). These discrepancies can be explained by sulfur oxidation coupled with abiotic reduction of Fe(III) and re-oxidation of Fe^{2+} within the root zone, respectively. Because *S. anglica* has a well-developed aerenchyma system and denser root systems, a large amount of O_2 can be readily supplied to deeper layers of SA sediment, stimulating re-oxidation of reduced compounds in the rhizosphere (i.e., Maricle and Lee, 2002; Koop-jakobsen and Wenzhöfer, 2015). Under this relatively sub-oxic condition, H_2S derived from SR (Eq. 1) is quickly oxidized by Fe(III) to form S^0 (Eq. 3, Ferreira et al., 2007; Jian et al., 2017). Simultaneously, the Fe^{2+} generated by microbial FeR (Eq. 2) and abiotic FeR (Eq. 3) is efficiently precipitated as FeS in the presence of H_2S (Eq. 4), which is then transformed to thermodynamically more stable pyrite (FeS_2) (Eq. 5; Canfield et al., 2005). The distribution of Fe–S compounds in pore water and the solid phase of the rhizosphere of SA were characterized by higher amounts of CRS and S^0 than those measured at SJ and UMF sites (**Figures 2**, 3). These results are consistent with the findings of Jian et al. (2017), who reported active sulfur oxidation in the rhizosphere of a mangrove system.

$$2CH_2O + SO_4{}^{2-} + 2H^+ = 2CO_2 + H_2S + 2H_2O \quad (1)$$

$$CH_2O + 4FeOOH + 8H^+ = CO_2 + 4Fe^{2+} + 7H_2O \quad (2)$$

$$4FeOOH + 3H_2S = 4Fe^{2+} + S^0 + S_2O_3{}^{2-} + 4H_2O \quad (3)$$

$$Fe^{2+} + H_2S = FeS + 2H^+ \quad (4)$$

$$FeS + S^0 = FeS_2 \; or \; FeS + H_2S = FeS_2 + H_2 \quad (5)$$

Depletion of H_2S coupled with the reduction of FeOOH via Eq. 3 at the rhizosphere of SA could also be explained by the abundance of sulfur-oxidizing bacteria (SOB) using S^0 as electron donors. Among the SOB, *Thioprofundaceae* in *Gammaproteobacteria* (γ-SOB), which use O_2 and $NO_3{}^-$ as electron acceptors and reduced sulfur (e.g., S^0, $S_2O_3{}^{2-}$, and $S_4O_6{}^{2-}$) as an electron donor, was predominant at SA, whereas *Sulfurovum* in *Epsilonproteobacteria* (ε-SOB) dominated at SJ (**Supplementary Table S1**). These notable differences suggest that the two SOB groups have distinctly different metabolic strategies for sulfur oxidation. The γ-SOB have a relatively narrow habitat zone because both oxygen and reduced sulfur are steadily supplied in their energy-producing pathway (Yamamoto and Takai, 2011; Ihara et al., 2017). In contrast, ε-SOB have versatile energy metabolisms in more reduced conditions. Thus, ε-SOB adapt to more dynamic and transient environmental conditions, such as hydrothermal system (Yamamoto and Takai, 2011; Ihara et al., 2017) and sulfidic finfish farm sediments (Choi et al., 2018). It is therefore plausible to identify γ-SOB dominating at the rhizosphere of SA, where both oxygen and reduced sulfur compounds (i.e., S^0 and $S_2O_3{}^{2-}$) are steadily supplied via aerenchyma of *S. anglica* and via Eq. (3) into rhizosphere, respectively.

Implications Associated With Climate Change

Temperature rise as a consequence of climate change has a significant impact on native and non-native plants in terms of photosynthesis, biomass allocation, and nutrient uptake in costal marshes and estuaries (Gray and Mogg, 2001; Loebl et al., 2006; Nehring and Hesse, 2008; Hulme, 2014). Because of a higher phenotypic plasticity compared with native plants, invasive plants would likely adapt more effectively to variations in environmental conditions resulting from climate change (Loebl et al., 2006; Charles and Dukes, 2009; Hulme, 2014; Grewell et al., 2016). For example, Loebl et al. (2006) suggested that the spread of invasive *S. anglica* was most likely triggered by temperature increase due to improved seed development. Similarly, Kirwan et al. (2009) demonstrated that an increase in annual temperature of 2–4°C would cause *S. alterniflora* productivity to increase by up to approximately 10–40%.

During the last 2–3 decades (1982–2006), warming rates (1°C per decade) of sea surface temperatures in the East Asian marginal seas, including the Yellow Sea and East China Sea, have been approximately 8 times faster than the global mean rate of 0.13°C per decade (Belkin, 2009). As a result, the current expansion of *S. anglica* observed in the Ganghwa intertidal sediments could be directly associated with the phenotypic plasticity of *S. anglica* under this climate change–induced warming trend. Our biogeochemical process studies combining microbiological analyses suggest that the invasion of *S. anglica*, which may displace native *S. japonica*, greatly alters the biogeochemical C–Fe–S cycles and associated microbial communities, which ultimately generates multi-directional variations in the ecological and biogeochemical processes of the coastal wetlands inhabited by native *S. japonica*. Our results provide scientific information that should be considered by decision-makers responsible for protecting estuarine and coastal environments in which invasive exotic plants have been established.

DATA AVAILABILITY STATEMENT

The datasets generated for this study can be found in the NCBI/PRJNA565620 (https://www.ncbi.nlm.nih.gov/bioproject/PRJNA565620/).

ETHICS STATEMENT

Written informed consent was obtained from the individuals for the publication of any potentially identifiable images or data included in this article.

AUTHOR CONTRIBUTIONS

S-UA, HC, and J-HH designed the study and wrote the manuscript. S-UA, U-JJ, BK, and HL collected the samples and performed most laboratory analysis. All the authors contributed to the discussion of the results and to the final version of the manuscript.

FUNDING

This research was supported by the Korean Long-term Marine Ecological Researches (K-LTMER) funded by the Korean Ministry of Oceans and Fisheries, and by the Mid-career Scientist Research Program funded by the Korean Ministry of Science and ICT (No. 2018R1A2B2006340).

SUPPLEMENTARY MATERIAL

The Supplementary Material for this article can be found online at: https://www.frontiersin.org/articles/10.3389/fmars.2020.00059/full#supplementary-material

REFERENCES

Alongi, D. M. (1998). *Coastal Ecosystem Processes*. Boca Raton, FL: CRC Press, 419.

Alongi, D. M., Tirendi, F., Dixon, P., Trott, L. A., and Brunskill, G. J. (1999). Mineralization of organic matter in intertidal sediments of a tropical semi-enclosed delta. *Estuar. Coast. Shelf Sci.* 48, 451–467. doi: 10.1006/ecss.1998.0465

An, S.-U., Mok, J.-S., Kim, S.-H., Choi, J.-H., and Hyun, J.-H. (2019). A large artificial dyke greatly alters partitioning of sulfate and iron reduction and resultant phosphorus dynamics in sediments of the Yeongsan River estuary, Yellow Sea. *Sci. Total Environ.* 665, 752–761. doi: 10.1016/j.scitotenv.2019.02.058

Armstrong, W., Cousins, D., Armstrong, J., Turner, D. W., and Beckett, P. M. (2000). Oxygen distribution in wetland plant roots and permeability barriers to gas-exchange with the rhizosphere: a microelectrode and modelling study with *Phragmites australis*. *Ann. Bot.* 86, 687–703. doi: 10.1006/anbo.2000.1236

Bang, J. H., and Lee, E. J. (2019). Differences in crab burrowing and halophyte growth by habitat types in a Korean salt marsh. *Ecol. Indic.* 98, 599–607. doi: 10.1016/j.ecolind.2018.11.029

Belkin, I. M. (2009). Rapid warming of large marine ecosystems. *Prog. Oceanogr.* 81, 207–213. doi: 10.1016/j.pocean.2009.04.011

Bertics, V. J., and Ziebis, W. (2009). Biodiversity of benthic microbial communities in bioturbated coastal sediments is controlled by geochemical microniches. *ISME J.* 3, 1269–1285. doi: 10.1038/ismej.2009.62

Bu, N., Qu, J., Li, Z., Li, G., Zhao, H., Zhao, B., et al. (2015). Effects of *Spartina alterniflora* invasion on soil respiration in the Yangtze River estuary, China. *PLoS One* 10:e0121571. doi: 10.1371/journal.pone.0121571

Canfield, D. E., Jørgensen, B. B., Fossing, H., Glud, R., Gundersen, J., Rasing, N. B., et al. (1993). Pathways of organic carbon oxidation in three continental margin sediments. *Mar. Geol.* 113, 27–40. doi: 10.1016/0025-3227(93)90147-N

Canfield, D. E., Thamdrup, B., and Kristensen, E. (2005). *Aquatic Geomicrobiology*. Amsterdam: Elsevier, 640.

Caporaso, J. G., Kuczynski, J., Stombaugh, J., Bittinger, K., Bushman, F. D., Costello, E. K., et al. (2010). QIIME allows analysis of high-throughput community sequencing data. *Nat. Methods* 7, 335–336. doi: 10.1038/nmeth.f.303

Charles, H., and Dukes, J. S. (2009). Effects of warming and altered precipitation on plant and nutrient dynamics of a New England salt marsh. *Ecol. Appl.* 19, 1758–1773. doi: 10.1890/08-0172.1

Cheng, X., Chen, J., Luo, Y., Henderson, R., An, S., Zhang, Q., et al. (2008). Assessing the effects of short-term *Spartina alterniflora* invasion on labile and recalcitrant C and N pools by means of soil fractionation and stable C and N isotopes. *Geoderma* 145, 177–184. doi: 10.1016/j.geoderma.2008.02.013

Choi, A., Cho, H., Kim, B., Kim, H. C., Jung, R., Lee, W., et al. (2018). Effects of finfish aquaculture on biogeochemistry and bacterial communities associated with sulfur cycles in highly sulfidic sediments. *Aquac. Environ. Interact.* 10, 413–427. doi: 10.3354/aei00278

Cline, J. D. (1969). Spectrophotometric determination of hydrogen sulfide in natural waters. *Limnol. Oceanogr.* 14, 454–458. doi: 10.4319/lo.1969.14.3.0454

Cook, P. L. M., Revill, A. T., Clementson, L. A., and Volkman, J. K. (2004). Carbon and nitrogen cycling on intertidal mudflats of a temperate Australian estuary. III. Sources of organic matter. *Mar. Ecol. Prog. Ser.* 280, 55–72. doi: 10.3354/meps280055

Cui, J., Chen, X. P., Nie, M., Fang, S. B., Tang, B. P., Quan, Z. X., et al. (2017). Effects of *Spartina alterniflora* invasion on the abundance, diversity, and community structure of sulfate reducing bacteria along a successional gradient of coastal salt marshes in China. *Wetlands* 37, 221–232. doi: 10.1007/s13157-016-0860-6

Dollhopf, S. L., Hyun, J.-H., Smith, A. C., Adams, H. J., O'Brien, S., and Kostka, J. E. (2005). Quantification of ammonia-oxidizing bacteria and factors controlling nitrification in salt marsh sediments. *Appl. Environ. Microbiol.* 71, 240–246. doi: 10.1128/AEM.71.1.240

Du, Z. –J., Wang, Z. –J., Zhao, J.-X., and Chen, G.-J. (2016). *Woeseia oceani* gen. nov., sp. nov., a chemoheterotrophic member of the order *Chromatiales*, and proposal of *Woeseiaceae* fam. nov. *Int. J. Syst. Evol. Microbiol.* 66, 107–112. doi: 10.1099/ijsem.0.000683

Fenchel, T., King, G. M., and Blackburn, T. H. (1998). *Bacterial Biogeochemistry: The Ecophysiology of Mineral Cycling*. San Diego, CA: Academic Press, 307.

Ferreira, T. O., Otero, X. L., Vidal-Torrado, P., and Macías, F. (2007). Effects of bioturbation by root and crab activity on iron and sulfur biogeochemistry in mangrove substrate. *Geoderma* 142, 36–46. doi: 10.1016/j.geoderma.2007.07.010

Fossing, H., Ferdelman, T. G., and Berg, P. (2000). Sulfate reduction and methane oxidation in continental margin sediments influenced by irrigation (South-East Atlantic off Namibia). *Geochim. Cosmochim. Acta* 64, 897–910. doi: 10.1016/S0016-7037(99)00349-X

Fossing, H., and Jørgensen, B. B. (1989). Measurement of bacterial sulfate reduction in sediments: evaluation of a single-step chromium reduction method. *Biogeochemistry* 8, 205–222. doi: 10.1007/BF00002889

Froelich, P. N., Klinkhammer, G. P., Bender, M. L., Luedtke, N. A., Heath, G. R., Cullen, D., et al. (1979). Early oxidation of organic matter in pelagic sediments of the eastern equatorial Atlantic: suboxic diagenesis. *Geochim. Cosmochim. Acta* 43, 1075–1090. doi: 10.1016/0016-7037(79)90095-4

Gao, G.-F., Li, P.-F., Zhong, J.-X., Shen, Z.-J., Chen, J., Li, Y.-T., et al. (2019). *Spartina alterniflora* invasion alters soil bacterial communities and enhances soil N_2O emissions by stimulating soil denitrification in mangrove wetland. *Sci. Total Environ.* 653, 231–240. doi: 10.1016/j.scitotenv.2018.10.277

Gray, A. J., and Mogg, R. J. (2001). Climate impacts on pioneer salt marsh plants. *Clim. Res.* 18, 105–112. doi: 10.3354/cr018105

Grewell, B. J., Castillo, J. M., Skaer Thomason, M. J., and Drenovsky, R. E. (2016). Phenotypic plasticity and population differentiation in response to salinity in the invasive cordgrass *Spartina densiflora*. *Biol. Invasions* 18, 2175–2187. doi: 10.1007/s10530-015-1041-x

Gribsholt, B., Kostka, J., and Kristensen, E. (2003). Impact of fiddler crabs and plant roots on sediment biogeochemistry in a Georgia saltmarsh. *Mar. Ecol. Prog. Ser.* 259, 237–251. doi: 10.3354/meps259237

Gribsholt, B., and Kristensen, E. (2002). Effects of bioturbation and plant roots on salt marsh biogeochemistry: a mesocosm study. *Mar. Ecol. Prog. Ser.* 241, 71–87. doi: 10.3354/meps241071

Gribsholt, B., and Kristensen, E. (2003). Benthic metabolism and sulfur cycling along an inundation gradient in a tidal *Spartina anglica* salt marsh. *Limnol. Oceanogr.* 48, 2151–2162. doi: 10.4319/lo.2003.48.6.2151

Hall, P. O. J., and Aller, R. C. (1992). Rapid, small-volume, flow injection analysis for CO_2, and NH_4^+ in marine and freshwaters. *Limnol. Oceanogr.* 37, 1113–1119. doi: 10.4319/lo.1992.37.5.1113

Haveman, S. A., DiDonato, R. J., Villanueva, L., Shelobolina, E. S., Postier, B. L., Xu, B., et al. (2008). Genome-wide gene expression patterns and growth requirements suggest that *Pelobacter carbinolicus* reduces Fe(III) indirectly via sulfide production. *Appl. Environ. Microbiol.* 74, 4277–4284. doi: 10.1128/AEM.02901-07

Hemminga, M. A., Huiskes, A. H. L., Steegstra, M., and van Soelen, J. (1996). Assessment of carbon allocation and biomass production in a natural stand of the salt marsh plant *Spartina anglica* using ^{13}C. *Mar. Ecol. Prog. Ser.* 130, 169–178. doi: 10.3354/meps130169

Hines, M. E. (1991). The role of certain infauna and vascular plants in the mediation of redox reactions in marine sediments. *Dev. Geochem.* 6, 275–286. doi: 10.1016/b978-0-444-88900-3.50031-x

Hines, M. E., Banta, G. T., Giblin, A. E., and Hobbie, J. E. (1994). Acetate concentrations and oxidation in salt−marsh sediments. *Limnol. Oceanogr.* 39, 140–148. doi: 10.4319/lo.1994.39.1.0140

Hines, M. E., Knollmeyer, S. L., and Tugel, J. B. (1989). Sulfate reduction and other sedimentary biogeochemistry in a northern New England salt marsh. *Limnol. Oceanogr.* 34, 578–590. doi: 10.4319/lo.1989.34.3.0578

Howarth, R. W., and Giblin, A. (1983). Sulfate reduction in the salt marshes at Sapelo Island. *Georgia Limnol. Oceanogr.* 28, 70–82. doi: 10.4319/lo.1983.28.1.0070

Hulme, P. E. (2014). Alien plants confront expectations of climate change impacts. *Trends Plant Sci.* 19, 547–549. doi: 10.1016/j.tplants.2014.05.003

Hyun, J.-H., Kim, S.-H., Mok, J.-S., Cho, H., Lee, T., Vandieken, V., et al. (2017). Manganese and iron reduction dominate organic carbon oxidation in deep continental margin sediments of the Ulleung Basin, East Sea. *Biogeosci. Discuss.* 14, 941–958. doi: 10.5194/bg-2016-222

Hyun, J.-H., Mok, J.-S., Cho, H.-Y., Kim, S.-H., Lee, K. S., and Kostka, J. E. (2009). Rapid organic matter mineralization coupled to iron cycling in intertidal mud flats of the Han River estuary, Yellow Sea. *Biogeochemistry* 92, 231–245. doi: 10.1007/s10533-009-9287-y

Hyun, J.-H., Smith, A. C., and Kostka, J. E. (2007). Relative contributions of sulfate- and iron(III) reduction to organic matter mineralization and process controls in contrasting habitats of the Georgia saltmarsh. *Appl. Geochem.* 22, 2637–2651. doi: 10.1016/j.apgeochem.2007.06.005

Ihara, H., Hori, T., Aoyagi, T., Takasaki, M., and Katayama, Y. (2017). Sulfur-oxidizing bacteria mediate microbial community succession and element cycling in launched marine sediment. *Front. Microbiol.* 8:152. doi: 10.3389/fmicb.2017.00152

Jensen, H. S., Mortensen, P. B., Andersen, F., Rasmussen, E., and Jensen, A. (1995). Phosphorus cycling in a coastal marine sediment, Aarhus Bay, Denmark. *Limnol. Oceanogr.* 40, 908–917. doi: 10.4319/lo.1995.40.5.0908

Jensen, M. M., Thamdrup, B., Rysgaard, S., Holmer, M., and Fossing, H. (2003). Rates and regulation of microbial iron reduction in sediments of the Baltic-North Sea transition. *Biogeochemistry* 65, 295–317. doi: 10.1023/A:1026261303494

Jian, L., Junyi, Y., Jingchun, L., Chongling, Y., Haoliang, L., and Spencer, K. L. (2017). The effects of sulfur amendments on the geochemistry of sulfur, phosphorus and iron in the mangrove plant (*Kandelia obovata* (S. L.)) rhizosphere. *Mar. Pollut. Bull.* 114, 733–741. doi: 10.1016/j.marpolbul.2016.10.070

Jiang, L. F., Luo, Y. Q., Chen, J. K., and Li, B. (2009). Ecophysiological characteristics of invasive *Spartina alterniflora* and native species in salt marshes of Yangtze River estuary, China. *Estuar. Coast. Shelf Sci.* 81, 74–82. doi: 10.1016/j.ecss.2008.09.018

Jørgensen, B. B. (1978). A comparison of methods for quantification of bacterial sulfate re duction in coastal marine sediment. I. Measurements with radiotracer technique. *Geomicrobiol. J.* 1, 11–27. doi: 10.1080/01490457809377721

Jørgensen, B. B. (2006). "Bacteria and marine biogeochemistry," in *Marine Geochemistry*, 2nd Edn, eds H. D. Schulz, and M. Zabel, (Berlin: Springer).

Kim, E., Kil, J., Joo, Y., and Jung, Y. (2015). Distribution and botanical characteristics of unrecorded alien weed *Spartina anglica* in Korea. *Weed Turfgrass Sci.* 4, 65–70. doi: 10.5660/wts.2015.4.1.65

Kim, J. (2016). A research review for establishing effective management practices of the highlay invasive cordgrass (*Spartina* spp.). *Weed Turfgrass Sci.* 5, 111–125. doi: 10.5660/wts.2016.5.3.111

King, J. K., Kostka, J. E., Frischer, M. E., Saunders, F. M., and Jahnke, R. A. (2001). A quantitative relationship that remonstrates mercury methylation rates in marine sediments are based on the community composition and activity of sulfate-reducing bacteria. *Environ. Sci. Technol.* 35, 2491–2496. doi: 10.1021/es001813q

Kirwan, M. L., Guntenspergen, G. R., and Morris, J. T. (2009). Latitudinal trends in *Spartina alterniflora* productivity and the response of coastal marshes to global change. *Glob. Chang. Biol.* 15, 1982–1989. doi: 10.1111/j.1365-2486.2008.01834.x

KOEM (2018). *Korea Marine EnviromentManagement Corporation-Marine Ecosystem Restoration*. Available at: https://www.koem.or.kr/site/koem/04/10401020000002019051004.jsp

Koo, B. J., Kwon, K. K., and Hyun, J.-H. (2005). The sediment-water interface increment due to the complex burrows of macrofauna in a tidal flat. *Ocean Sci. J.* 40, 221–227. doi: 10.1007/BF03023522

Koo, B. J., Kwon, K. K., and Hyun, J.-H. H. (2007). Effect of environmental conditions on variation in the sediment-water interface created by complex macrofaunal burrows on a tidal flat. *J. Sea Res.* 58, 302–312. doi: 10.1016/j.seares.2007.07.002

Koop-Jakobsen, K., Mueller, P., Meier, R. J., Liebsch, G., and Jensen, K. (2018). Plant-sediment interactions in salt marshes–an optode imaging study of O_2, pH, and CO_2 gradients in the rhizosphere. *Front. Plant Sci.* 9:541. doi: 10.3389/fpls.2018.00541

Koop-jakobsen, K., and Wenzhöfer, F. (2015). The dynamics of plant-mediated sediment oxygenation in *Spartina anglica* rhizospheres–a planar optode study. *Estuaries Coast.* 38, 951–963. doi: 10.1007/s12237-014-9861-y

Koretsky, C. M., Haveman, M., Cuellar, A., Beubing, L., Shattuck, T., and Wagner, M. (2008). Influence of *Spartina* and *Juncus* on saltmarsh sediments. I. Pore water geochemistry. *Chem. Geol.* 255, 87–99. doi: 10.1007/s00248-015-0651-2

Koretsky, C. M., Moore, C., Meile, C., Dichristina, T., and Van Cappellen, P. (2003). Seasonal oscillations in microbial iron and sulfate reduction in saltmarsh sediments (Sapelo Island, GA, USA). *Biogeochemistry* 64, 179–203.

Kostka, J. E., Gribsholt, B., Petrie, E., Dalton, D., Skelton, H., and Kristensen, E. (2002a). The rates and pathways of carbon oxidation in bioturbated saltmarsh sediments. *Limnol. Oceanogr.* 47, 230–240. doi: 10.4319/lo.2002.47.1.0230

Kostka, J. E., and Luther, G. W. (1994). Partitioning and speciation of solid-phase iron in salt-marsh sediments. *Geochim. Cosmochim. Acta* 58, 1701–1710. doi: 10.1016/0016-7037(94)90531-2

Kostka, J. E., Roychoudhury, A., and Van Cappellen, P. (2002b). Rates and controls of anaerobic microbial respiration across spatial and temporal gradients in saltmarsh sediments. *Biogeochemistry* 60, 49–76.

Kristensen, E., and Alongi, D. M. (2006). Control by fiddler crabs (*Uca vocans*) and plant roots (*Avicennia marina*) on carbon, iron, and sulfur biogeochemistry in mangrove sediment. *Limnol. Oceanogr.* 51, 1557–1571. doi: 10.4319/lo.2006.51.4.1557

Kristensen, E., and Kostka, J. E. (2005). "Macrofaunal burrows and irrigation inmarine sediment: microbiological and biogeochemical interactions," in *Interaction Between Macro- and Microorganisms in Marine Sediments*, Vol. 60, eds E. Kristensen, R. R. Haese, and J. E. Kostka, (Washington, DC: American Geophysical Union), 125–157. doi: 10.1029/ce060p0125

Kristensen, E., Mangion, P., Tang, M., Flindt, M. R., Holmer, M., and Ulomi, S. (2011). Microbial carbon oxidation rates and pathways in sediments of two Tanzanian mangrove forests. *Biogeochemistry* 103, 143–158. doi: 10.1007/s10533-010-9453-2

Lee, R. W. (2003). Physiological adaptations of the invasive cordgrass *Spartina anglica* to reducing sediments: rhizome metabolic gas fluxes and enhanced O_2 and H_2S transport. *Mar. Biol.* 143, 9–15. doi: 10.1007/s00227-003-1054-3

Li, B., Liao, C. H., Zhang, X. D., Chen, H. L., Wang, Q., Chen, Z. Y., et al. (2009). *Spartina alterniflora* invasions in the Yangtze River estuary, China: an overview of current status and ecosystem effects. *Ecol. Eng.* 35, 511–520. doi: 10.1016/j.ecoleng.2008.05.013

Li, W., Fu, L., Niu, B., Wu, S., and Wooley, J. (2012). Ultrafast clustering algorithms for metagenomic sequence analysis. *Brief. Bioinform.* 13, 656–668. doi: 10.1093/bib/bbs035

Liao, C., Luo, Y., Jiang, L., Zhou, X., Wu, X., Fang, C., et al. (2007). Invasion of *Spartina alterniflora* enhanced ecosystem carbon and nitrogen stocks in the Yangtze estuary, China. *Ecosystems* 10, 1351–1361. doi: 10.1007/s10021-007-9103-2

Liesack, W., and Finster, K. (1994). Phylogenetic analysis of five strains of gram-negative, obligately anaerobic, sulfur-reducing bacteria and description of *Desulfuromusa* gen. nov., including *Desulfuromusa kysingii* sp. nov., *Desulfuromusa bakii* sp. nov., and *Desulfuromusa succinoxidans* sp. nov. *Int J Syst bacteriol.* 44, 753–758. doi: 10.1099/00207713-44-4-753

Loebl, M., Van Beusekom, J. E. E., and Reise, K. (2006). Is spread of the neophyte *Spartina anglica* recently enhanced by increasing temperatures? *Aquat. Ecol.* 40, 315–324. doi: 10.1007/s10452-006-9029-3

Lovell, C. R. (2005). "Belowground interactions among salt marsh plants and microorganisms," in *Interactions Between Macro- and Microorganisms in Marine Sediments*, eds E. Kristensen, R. R. Haese, and J. E. Kostka, (Washington, DC: American Geophysical Union), 61–84.

Luo, M., Liu, Y., Huang, J., and Xiao, L. (2018). Rhizosphere processes induce changes in dissimilatory iron reduction in a tidal marsh soil: a rhizobox study. *Plant Soil.* 433, 83–100. doi: 10.1007/s11104-018-3827-y

Luo, M., Zeng, C. S., Tong, C., Huang, J. F., Chen, K., and Liu, F. Q. (2016). Iron reduction along an inundation gradient in a Tidal Sedge (*Cyperus malaccensis*) marsh: the rates, pathways, and contributions to anaerobic organic matter mineralization. *Estuaries Coast.* 39, 1679–1693. doi: 10.1007/s12237-016-0094-0

Maricle, B. R., and Lee, R. W. (2002). Aerenchyma development and oxygen transport in the estuarine cordgrasses *Spartina alterniflora* and *S. anglica*. *Aquat. Bot.* 74, 109–120. doi: 10.1016/S0304-3770(02)00051-7

McLeod, E., Chmura, G. L., Bouillon, S., Salm, R., Björk, M., Duarte, C. M., et al. (2011). A blueprint for blue carbon: toward an improved understanding of the role of vegetated coastal habitats in sequestering CO_2. *Front. Ecol. Environ.* 9:552–560. doi: 10.1890/110004

Mok, J.-S., Kim, S.-H., Kim, J., Cho, H., An, S.-U., Choi, A., et al. (2019). Impacts of typhoon-induced heavy rainfalls and resultant freshwater runoff on the partitioning of organic carbon oxidation and nutrient dynamics in the intertidal sediments of the Han River estuary, Yellow Sea. *Sci. Total Environ.* 691, 858–897. doi: 10.1016/j.scitotenv.2019.07.031

Nehring, S., and Hesse, K. J. (2008). Invasive alien plants in marine protected areas: the *Spartina anglica* affair in the European Wadden Sea. *Biol. Invasions* 10, 937–950. doi: 10.1007/s10530-008-9244-z

Odum, E. P. (2000). "Tidal marshes as outwelling/pulsing systems," in *Concepts and Controversies in Tidal Marsh Ecology*, eds M. P. Weinstein, and D. A. Kreeger, (Dordrecht: Kluwer Academic Publishers), 3–7. doi: 10.1007/0-306-47534-0_1

Parsons, T. R., Maita, Y., and Lalli, C. M. (1984). *A Manual of Chemical and Biological Methods for Seawaer Analysis*. Oxford: Pergamon Press, 173.

Phillips, E. J. P., and Lovley, D. R. (1987). Determination of Fe(III) and Fe(II) in oxalate extracts of sediment. *Soil Sci. Soc. Am. J.* 51, 938–941. doi: 10.2136/sssaj1987.03615995005100040021x

Quintana, C. O., Shimabukuro, M., Pereira, C. O., Alves, B. G. R., Moraes, P. C., Valdemarsen, T., et al. (2015). Carbon mineralization pathways and bioturbation in coastal Brazilian sediments. *Sci. Rep.* 5:16122. doi: 10.1038/srep16122

Schloss, P. D., Westcott, S. L., Ryabin, T., Hall, J. R., Hartmann, M., Hollister, E. B., et al. (2009). Introducing mothur: open-source, platform-independent, community-supported software for describing and comparing microbial communities. *Appl. Environ. Microbiol.* 75, 7537–7541. doi: 10.1128/AEM.01541-09

Stookey, L. L. (1970). Ferrozine-a new spectrophotometric reagent for iron. *Anal. Chem.* 42, 779–781. doi: 10.1021/ac60289a016

Sundby, B., Vale, C., Caetano, M., and Luther, G. W. III (2003). Redox chemistry in the root zone of a salt marsh sediment in the Tagus estuary, Portugal. *Aquat. Geochem.* 9, 257–271. doi: 10.1023/B:AQUA.0000022957.42522.9a

Thamdrup, B., and Canfield, D. E. (1996). Pathways of carbon oxidation in continental margin sediments off central Chile. *Limnol. Oceanogr.* 41, 1629–1650. doi: 10.4319/lo.1996.41.8.1629

Thomas, F., Giblin, A. E., Cardon, Z. G., and Sievert, S. M. (2014). Rhizosphere heterogeneity shapes abundance and activity of sulfur-oxidizing bacteria in vegetated salt marsh sediments. *Front. Microbiol.* 5:309. doi: 10.3389/fmicb.2014.00309

Vandieken, V., Mußmann, M., Niemann, H., and Jørgensen, B. B. (2006). *Desulfuromonas svalbardensis* sp. nov. and *Desulfuromusa ferrireducens* sp. nov., psychrophilic, Fe(III)-reducing bacteria isolated from Arctic sediments, Svalbard. *Int. J. Syst. Evol. Microbiol.* 56, 1133–1139. doi: 10.1099/ijs.0.63639-0

Vandieken, V., Pester, M., Finke, N., Hyun, J.-H., Friedrich, M. W., Loy, A., et al. (2012). Three manganese oxide-rich marine sediments harbor similar communities of acetate-oxidizing manganese-reducing bacteria. *ISME J.* 6, 2078–2090. doi: 10.1038/ismej.2012.41

Wang, W., Sardans, J., Wang, C., Zeng, C., Tong, C., Chen, G., et al. (2019). The response of stocks of C, N, and P to plant invasion in the coastal wetlands of China. *Glob. Change Biol.* 25, 733–743. doi: 10.1111/gdb.14491

Weiss, J. V., Emerson, D., Backer, S. M., and Megonigal, J. P. (2003). Enumeration of Fe (II) -oxidizing and Fe (III)-reducing bacteria in the root zone of wetland plants: implications for a rhizosphere iron cycle. *Biogeochemistry* 64, 77–96. doi: 10.1023/A:1024953027726

Woo, H. J., and Je, J.-G. (2002). Changes of sedimentary environments in the southern tidal flat of Ganghwa Island. *Ocean Polar Res.* 24, 331–343. doi: 10.4217/opr.2002.24.4.331

Yamamoto, M., and Takai, K. (2011). Sulfur metabolisms in epsilon-and gamma-*Proteobacteria* in deep-sea hydrothermal fields. *Front. Microbiol.* 2:192. doi: 10.3389/fmicb.2011.00192

Yang, W., Zhao, H., Chen, X. L., Yin, S. L., Cheng, X. L., and An, S. Q. (2013). Consequences of short-term C4 plant *Spartina alterniflora* invasions for soil organic carbon dynamics in a coastal wetland of Eastern China. *Ecol. Eng.* 61, 50–57. doi: 10.1016/j.ecoleng.2013.09.056

Yuan, J. J., Ding, W. X., Liu, D. Y., Kang, H. J., Xiang, J., and Lin, Y. X. (2016). Shifts in methanogen community structure and function across a coastal marsh transect: effects of exotic *Spartina alterniflora* invasion. *Sci. Rep.* 6:18777. doi: 10.1038/srep18777

Zhang, G., Bai, J., Jia, J., Wang, W., Wang, X., Zhao, Q., et al. (2019). Shifts of soil microbial community composition along a short-term invasion chronosequence of *Spartina alterniflora* in a Chinese estuary. *Sci. Total Environ.* 657, 222–233. doi: 10.1016/j.scitotenv.2018.12.061

Zhang, P., Nie, M., Li, B., and Wu, J. (2017). The transfer and allocation of newly fixed C by invasive *Spartina alterniflora* and native *Phragmites australis* to soil microbiota. *Soil Biol. Biochem.* 113, 231–239. doi: 10.1016/j.soilbio.2017.06.003

Zhang, Q. F., Peng, J. J., Chen, Q., Yang, X. R., Hong, Y. W., and Su, J. Q. (2013). Abundance and composition of denitrifiers in response to *Spartina alterniflora* invasion in estuarine sediment. *Can. J. Microbiol.* 59, 825–836. doi: 10.1139/cjm-2013-0516

Zopfi, J., Ferdelman, T. G., and Fossing, H. (2004). Distribution and fate of sulfur intermediates—sulfite, tetrathionate, thiosulfate, and elemental sulfur-in marine sediments. *Geol. Soc. Am. Spec. Pap.* 379, 97–116. doi: 10.1130/0-8137-2379-5.97

Conflict of Interest: The authors declare that the research was conducted in the absence of any commercial or financial relationships that could be construed as a potential conflict of interest.